

Optimizing Heat Exchanger Design Through Emerging Computational Fluid Dynamics Methods

Vikash Singh Patel

M.Tech Scholar

Department of Mechanical
Engineering

Technocrats Institute of Technology
and Science, RGPV

Bhopal, Madhya Pradesh, India

vikashsingh2604@gmail.com

Dr. Ankit Goyal

Professor

Department of Mechanical
Engineering,

Technocrats Institute of Technology
and Science, RGPV

Bhopal, Madhya Pradesh, India

Prof. Priyavrat Kumar

Assistant Professor

Department of Mechanical
Engineering

Technocrats Institute of Technology
and Science, RGPV

Bhopal, Madhya Pradesh, India

Abstract: This study carries out a detailed CFD analysis of a concentric triple-tube heat exchanger to investigate the thermal performance for different configurations and nanofluid concentrations of 0.0% and 0.1%. The investigation covers heat transfer rates, temperature distributions, and fluid flow dynamics in three different setups: baffle-less operation, straight baffles, and baffles inclined at 45°. Parameters analyzed are the inlet and outlet temperatures, specific heat, and the overall heat transfer coefficient for system efficiency. The results indicated that nanofluid concentration played a critical role in thermal performance. With a 0.1% concentration, heat transfer efficiency is highly improved. In configurations, the inclined baffle at 45° angle yields the highest thermal efficiency because temperature gradients are optimized, and fluid turbulence is increased. The results of this study have the potential for advanced baffle designs and nanofluids in efficient heat exchanger performance. This study has provided valuable insight into the optimization of heat exchanger designs to improve energy efficiency in industrial applications. Future research can further explore additional nanofluid types and advanced geometrical modifications to further enhance performance.

Keywords: Computational Fluid Dynamics (CFD), concentric triple-tube heat exchanger, nanofluids, thermal performance, heat transfer efficiency, inclined baffles, energy efficiency, fluid dynamics.

I. Introduction

Heat exchangers are one of the most critical equipment in the process of energy transfer between fluids through conduction without physical mixing, and every industry, from power plants to refrigerator and heating and air conditioning applications, needs it. Among all other types, the triple-tube heat exchanger is notable for its particular design, where a multiplicity of fluid streams can transfer heat together, different from the conventional shell-and-tube or plate type heat exchanger. This makes it ideal for application-specific, very precise thermal control applications like chemical processing, food and beverage manufacture, and pharmaceutical applications. The compact structure is meant to optimize use of space; reduce the need for materials in general, helping meet sustainability targets; and accounts for the trend in more and more advanced industries [1, 2]. Heat exchangers are crucial parts of a thermal system. They allow heat transfer from at least two fluids without mixing. This feature is largely applied in various industries, which enhance efficient thermal energy use. In power generation, heat exchangers aid energy transfer in steam turbines, in which

the heat from burning fuel is transferred to water or other working fluids to create steam that drives turbines and generates electricity. Such systems also recover excessive thermal energy, leading to higher efficiency and reduced cost, which benefits sustainable energy generation [3]. Heat exchangers find crucial application in industrial fields in the safe and efficient execution of chemical reactions within petrochemical industries, in hygienic processing and quality products within food and beverages, and maintaining uniform temperature processes in the casting of metals and plastics production. Their ability to maintain thermal equilibrium enhances process efficiency, reduces equipment downtime, and extends the lifespan of machinery [4].

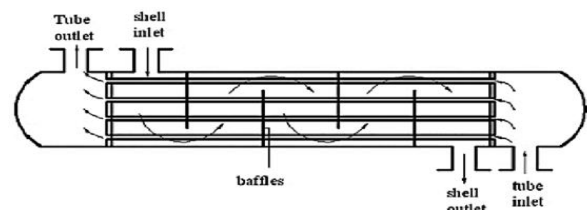


Figure 1 Shell and tube heat exchanger [7]

Heat exchangers play an indispensable role in modern thermal systems to ensure both energy conservation and environmental sustainability. Most renewable energy technologies, from solar thermal and geothermal systems, heavily rely on heat exchangers to operate efficiently. For example, in a solar thermal system, they transfer the heat of fluids heated by solar radiation to the water or steam system to achieve energy storage and power generation. Another example is in geothermal systems, where efficient heat transfer from underground reservoirs to buildings minimizes the harmful effects on the environment [5]. Computational tools and materials science have fostered breakthroughs in compact high-performance heat exchangers which could survive extreme conditions. Such innovations are testament to the centrality of heat exchangers in building future sustainable and energy-efficient thermal systems [6, 7].

A. Triple Tube Heat Exchangers

Triple-tube heat exchangers are advanced thermal devices that are meant to enhance efficiency and handle complex operating conditions. Unlike conventional heat exchangers

with two fluid streams, the triple-tube exchanger features an additional concentric tube that allows three fluid streams to interact simultaneously. This configuration maximizes the heat transfer surface area and provides greater flexibility in thermal management. Flow configurations containing either parallel flow or counter-flow, or even a hybrid, are better suited for applications requiring compact designs and high efficiency. Layered configurations permit conduction among fluids at different temperature levels for use in high-thermal-gradient-industries processes, precise heating or cooling chemical or pharmaceutical applications, which require product quality assurance and safety. In addition, their compact size is advantageous for spatially restricted spaces [8, 9]. Triple-tube heat exchangers possess high heat transfer coefficients and are capable of functioning effectively under different flow conditions. They therefore exhibit excellent thermal performance by minimizing input energy requirements and maximizing output efficiency due to full utilization of the available surface area. They are fluid handling devices which can handle fluids with different viscosities and phases, thereby suited for food processing industries where control of thermal activity is critical in terms of product quality and safety.

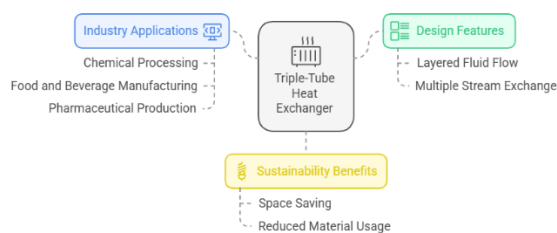


Figure 2 Triple-Tube Heat Exchanger

Their design is also amenable to ease of maintenance and long life, due to features like a concentric tube structure that allows for easy inspection and cleaning-an important factor for hygiene-sensitive industries. Improvements in materials and manufacturing processes have enhanced their corrosion and fouling resistance, minimizing maintenance and maximizing service life. As the industrial world increasingly emphasizes efficient, environmentally conscious thermal management solutions, the triple-tube heat exchanger continues to be one of the most versatile and sustainable solutions available for industrial applications [10, 11, 12].

B. Working principle of triple tube Heat Exchangers

The triple-tube heat exchanger works based on the concept of indirect transfer of heat where energy is exchanged between three fluid streams simultaneously, without direct mixing. It is composed of three concentric tubes that allow for heat transfer through the walls separating the inner, middle, and outer annular regions carrying fluids of different temperatures. The design of the triple tube supports parallel, counterflow, or mixed configurations with maximum thermal efficiency and adaptability in diverse applications. Being highly adaptable for fluids with different viscosities, phases, and temperatures, the triple-tube exchanger is very suitable for industries such as

chemical processing, pharmaceuticals, food, and beverages because it affords industries complex thermal demands and compact, efficient designs. The ability to manage multiple streams within a single unit helps in conserving space, reducing material use, and being cost-effective while meeting high performance and reliability standards [13, 14].

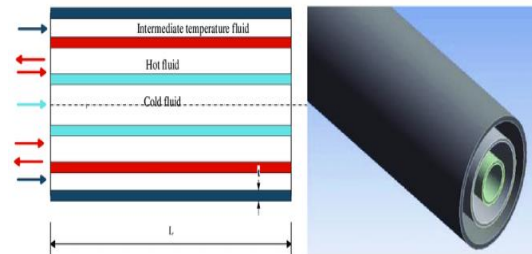


Figure 3 Schematic representation of Triple Concentric-tube Heat exchanger and its Computational domain [14]

C. Application of Triple Tube Concentric Heat Exchanger

Triple concentric tube heat exchangers offer far better performance compared to the shell-and-tube configuration because they enhance the efficiency of heat transfer and are flexible. The design is such that there is an increased heat exchange surface area compared to their length, resulting in higher coefficients of heat transfer and better performance. The three-tube system also facilitates the transfer of heat between three fluids, thus finding applications in industries such as food processing, pasteurization, refrigeration, and freezing where thermal efficiency needs to be quite high [15, 16].

Recent advancements such as compact and curved pipe designs, including helium-hardened tubes, have further enhanced the function of exchangers by optimizing fluid flow and reducing thermal resistance. Nanofluids-engineered liquids that contain nanoparticles-have brought about increase in thermal conductivity and overall heat transfer, eliminating limitations of traditional fluids, proving to be useful for high-demand applications where superior thermal performance is sought after [17, 18]. Heat transfer is enhanced both by active and passive techniques. The former includes methods such as rotating surfaces or impinging jets that increase heat transfer, but the approach is cumbersome and expensive. In contrast, methods like turbulators, wire coil inserts, or twisted tape designs are more feasible and economical to deploy and create turbulence and therefore heat transfer enhancement without adding power. Innovations in the form of advanced heat pipe configurations, turbulence-enhancing modifications, and nanofluid integration ensure that triple concentric tube heat exchangers remain a reliable and energy-efficient solution to modern thermal management demands [19-23].

II.LITERATURE REVIEW

Malika and Sonawane (2024) [24] assessed the cost model and environmental impact of shell and tube heat exchangers (STHE) at the early design stage. They compared the performance of a nanofluid-enhanced system with standard STHE using lifecycle analysis (LCA). Results indicated that 0.5 vol% TiO₂-SiC/water hybrid nanofluid enhanced

the heat transfer efficiency by increasing the Nusselt number by 65% and pressure drop by 8% compared to water. The ANN was applied to evaluate the ecological impact and cost, and the IdematLightLCA software was used to calculate energy, carbon footprint, and lifetime costs. Although the payback period was longer, the nanofluid-based system was more economical and environmentally sustainable over its lifetime.

A hybrid analytical-experimental algorithm has been developed by **Abdollahpour and Darbandi (2024) [25]** for optimizing the hydrothermal performance of shell-and-tube heat exchangers to find the optimal tube and baffle combinations. The hydraulic diameter was most valuable for compact STHes where size is limited. Enhancement in performance, based on dimpled-tube and disc-doughnut baffles as compared to the base STH with smooth-tube and segmental baffles, is predicted by the algorithm. The algorithm has been verified against experimental and numerical data, thus enabling fast performance evaluation under various operating conditions. Results indicated that the mean heat transfer rate for dimpled tubes with segmental or disc-doughnut baffles was increased by 15.6% and 22.4%, respectively.

Ghalandari et al. (2021) [26] outlined the important role that intelligent methods had in the precise forecasting of heat exchanger performance, in turn providing quicker alternatives to experimental and computational approaches. The efficiency of machine learning models in the given context depends on factors like algorithm architecture, input variables, and system complexity. Review of the study is mainly related to several applications of intelligent methods in heat exchanger modeling, summarizing key findings, and considerations that draw out factors influencing them. Recommendations for future research were also given to further improve the accuracy and applicability of these approaches.

Wang et al. (2024) [27] carried out a numerical investigation on EHD-mediated wavy channels with heat transfer characteristics that contrasted with those of straight channels. Optimum heat transfer across continuous wavy channels was attained when a single electrode was placed above the crest. Design strategies for aligning electrodes for continuous and discontinuous wavy channels were presented, bringing to light the importance of the ratio of the horizontal section length to wavelength, l/λ , for enhancement in heat transfer. In discontinuous channels, the electrodes should be located at intersections of wave-horizontal sections. In optimum performance, electrode spacing must be maximized when $l/\lambda < 0.15$ and minimized when $l/\lambda > 0.15$ to decrease barrier effects.

According to **Guo et al. (2023) [28]**, integrated polymer composites for electronics are critical due to severe heat collection as well as electromagnetic wave (EMW) radiation, concerning efforts to miniaturize the dimensions of 5G devices. The said conventional approaches that remain too focused on either thermal conduction or EMW absorption cannot satisfy these needs. The paper covered new approaches and functional fillers in developing composites with both characteristics. It reviewed recent trends, performance influencers, underlying mechanisms,

challenges, and possible solutions and aimed to guide the development of multifunctional polymer composites for advanced electronics.

Wu et al. (2020) [29] highlighted phase change materials (PCMs) as efficient energy storage due to their high energy density and stability. The paper discussed PCM morphology, preparation, and phonon-based thermal conduction, including phonon-phonon, phonon-defect, and phonon-boundary scattering. Additives such as MOFs, graphene foam, and HBN nanoparticles enhance thermal conductivity by widening the pathways of heat transfer. However, much work is still required to optimize the performance of PCMs and develop efficient heat storage systems for solar and industrial applications.

III.OBJECTIVES

This project revolves around the design and development of an adaptable triple concentric tube heat exchanger with the following major goals:

- Investigate how various heat exchanger types are governed by mathematical relationships.
- Explore and compare the different triple concentric tube heat exchanger designs' performance results.
- Every triple concentric tube heat exchanger design should undergo a Computational Fluid Dynamics (CFD) analysis at different nanofluid concentrations.
- Create computer simulations of triple concentric tube heat exchangers, considering designs with and without baffles as well as those with and without inclined baffles.

IV.METHODOLOGY

The study focused on a detailed investigation into the thermal dynamics of the concentric triple tube heat exchanger with specific reference to the cooling functions it serves. The investigation revolves around the flow and thermal performances of the cold fluids carried in the inner and outer tubes. Starting initially at different temperatures, namely $T_{c1(out)}$ in the case of the inner tube and $T_{c2(out)}$ in that of the outer tube. These fluids are passed through the exchanger; they experience contact with ambient thermal conditions, causing adjustments in temperatures by their exit points to $T_{c1(in)}$ and $T_{c2(in)}$, respectively. This temperature shift, along with variables of influence, can be deciphered using an integrated mathematical framework for a deep insight into heat transfer processes and cooling mechanisms. This approach provides critical insights into the exchanger's performance, offering a foundation for advancing the design and efficiency of future heat exchanger systems.

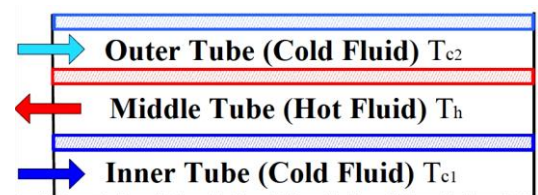


Figure 4 Fluid Flow Configuration in a Triple-Tube Heat Exchanger

The hot fluid requiring cooling is introduced into the inner annulus of the triple-tube heat exchanger, entering at a temperature denoted as $T_{h(in)}$ and exiting at $T_{h(out)}$, as depicted in figure 4. A counterflow configuration of a triple-tube heat exchanger, with hot fluid in the center tube and opposite directions for cold fluids within the inner and outer tubes, has been considered. The rationale is based on its suitability for uniform temperature gradients throughout the exchanger's length and for ensuring the possibility of effective and high-quality heat transfer, thus being accurate for precise temperature control. Since this design ensures optimal thermal performance by maximizing the temperature difference between fluids, it is suitable for applications such as HVAC systems and industrial processes. For simplicity, it is assumed that the fluid properties are constant while considering steady-state conditions, no phase changes, incompressible fluids, and effective insulation to prevent external heat loss. The use of energy balance equations then analyses the heat transfer behavior of the system under such controlled conditions, offering crucial information in optimizing performance.

$$v = \frac{Re \times \mu}{\rho \times D_{inner}} \quad (1)$$

$$\dot{m} = \rho \times A_{cross\ section} \times v \quad (2)$$

Here v is the velocity in m/s, μ is dynamic viscosity in kg/m·s, ρ the fluid density is measured in kg/m³, D_{inner} is the diameter of the inner tube in meters. The mass flow rate for the Reynolds number Re is given as \dot{m} by kg/s while the cross-sectional area is expressed as $A_{cross\ section}$ measured in m².

The rate of heat transfer between a hot nanofluid, a cool fluid, and a normal fluid

$$q_{nf} = \dot{m}_{nf} \cdot c_{p,nf} (T_{nf,in} - T_{nf,out}) \quad (3)$$

$$q_{cold} = \dot{m}_{cold} \cdot c_{p,cold} (T_{cold,out} - T_{cold,in}) \quad (4)$$

$$q_{normal} = \dot{m}_{normal} \cdot c_{p,normal} (T_{normal,out} - T_{normal,in}) \quad (5)$$

The variables are heat transfer rates q_{nf} , q_{cold} and specific heat capacities (q_{nf} , q_{cold} , q_{normal}) for hot nanofluid, cold fluid, and standard/normal fluid, respectively, along with their mass flow rates (\dot{m}_{nf} , \dot{m}_{cold} , \dot{m}_{normal}). Temperatures include the inlet and outlet conditions for hot nanofluid ($T_{nf,in} - T_{nf,out}$), cold fluid ($T_{cold,out} - T_{cold,in}$), and normal fluid ($T_{normal,out} - T_{normal,in}$).

The concentric triple tube heat exchanger's overall heat transfer coefficient

$$U = \frac{q_h}{A_{cross,inner} \times LMTD_{avg}} \quad (6)$$

$$LMTD_{avg} = \frac{LMTD_{hot\&\ cold} + LMTD_{hot\&\ nf}}{2} \quad (7)$$

The variables are total heat transfer coefficient (U), inner tube surface area ($A_{cross,inner}$), and average logarithmic mean temperature difference ($LMTD_{avg}$). The $LMTD$ is defined for two different conditions; one is the hot and cold

fluids ($LMTD_{hot\&\ cold}$), and the other is the hot fluid and nanofluid ($LMTD_{hot\&\ nf}$).

Average Temperature of the Cold Fluid Stream

$$T_{b,cold} = \frac{T_{cold-1,in} + T_{cold-1,out}}{2} \quad (8)$$

$$T_{b,hot} = \frac{T_{hot,in} + T_{hot,out}}{2} \quad (9)$$

The variables represent the temperatures of the fluids in a heat exchanger:

$T_{cold-1,out}$ and $T_{cold-1,in}$ denote the outlet and inlet temperatures of the cold fluid, respectively, while $T_{b,cold}$ is the cold fluid's bulk mean temperature. Similarly, $T_{hot,in}$ and $T_{hot,out}$ indicate the inlet and outlet temperatures of the hot fluid, with $T_{b,hot}$ representing the hot fluid's bulk mean temperature.

Linear velocity

Linear velocity of nano fluid

$$v_{nf} = \frac{\dot{m}_{nf}}{\rho_{nf} A_{cross\ mid}} \text{ m/sec} \quad (10)$$

Where

\dot{m}_{nf} = Nano-fluid's mass flow rate

v_{nf} = Nano-fluid's linear velocity

$A_{cross\ mid}$ = Middle tube's cross section area

ρ_{nf} = Density of nano-fluid

Linear velocity of cold water

$$v_{cold} = \frac{\dot{m}_{cold}}{\rho_{cold} A_{cross\ inner}} \text{ m/sec} \quad (11)$$

Where

v_{cold} = Linear velocity of cold water

\dot{m}_{cold} = mass flow rate of cold water

ρ_{cold} = Density of cold fluid

$A_{cross\ inner}$ = Inner tube's cross sectional area

Linear velocity of normal water

$$v_{normal} = \frac{\dot{m}_{normal}}{\rho_{normal} A_{cross\ outer}} \text{ m/sec}$$

Where

\dot{m}_{normal} = mass flow rate of normal water

v_{normal} = Linear velocity of normal water

$A_{cross\ outer}$ = Outer tube's cross sectional area

ρ_{normal} = Density of normal water

Reynolds Number

Reynolds Number of GNPs

$$Re_{e,nf} = \frac{\rho_{nf} v_{nf} D_{mid}}{\mu_{nf}} \quad (12)$$

Where

$Re_{e,nf}$ = Nano-Fluid Reynolds Number

D_{mid} = Diameter of middle tube

μ_{nf} = Nano-fluid's kinematic viscosity

Reynolds Number of normal water

$$Re_{e,normal} = \frac{\rho_{normal} v_{normal} D_{out}}{\mu_{normal}} \quad (13)$$

Where

μ_{normal} = Normal water's kinematic viscosity

$Re_{e,normal}$ = Reynolds number of normal water

D_{out} = Outer tube diameter

Reynolds Number of cold water

$$Re_{cold} = \frac{\rho_{cold} v_{cold} D_{inner}}{\mu_{cold}} \tag{14}$$

Where

Re_{cold} = Cold water's reynolds number

ρ_{cold} = Cold water density

D_{inner} = Inner tube's diameter

Calculation of GNPs' Nusselt number:

$$Nu_{nf} = \frac{h_{nf} D_{h,nf}}{k_{nf}} = 0.023 Re_{nf}^{0.8} \times Pr_{nf}^{0.4} \tag{15}$$

Where

Nu_{nf} = Nano-fluid's Nusselt number

k_{nf} = Nano-fluid's Thermal conductivity

h_{nf} = Nano-fluid's convective coefficient

$D_{h,nf}$ = Nano-fluid's Hydraulic diameter of nano-fluid

Pr_{nf} = Nano-fluid's Prandelt number

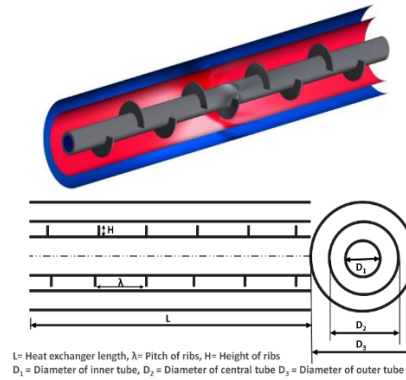


Figure 5 Concentric triple tube heat exchanger's conceptual diagram

Water properties are provided in SI units for the temperature range of 0°C to 100°C at a standard atmospheric pressure of 101.325 kPa

Table 1: Water properties at atmospheric pressure

water Temperature [°C]	Density (ρ) [kg/m ³]	Dynamic Viscosity (μ) (Ns/m ²) x10 ⁻³	Specific Heat (c _p) kJ/kg.K	Prandtl Number (Pr)	Kinematic Viscosity (ν) (m ² /s ²)x10 ⁶	Thermal conductivity (k) [W/m K] x10 ³
0.000	987.840	1.580	4.210	12.480	1.700	0.680
5.000	987.970	1.440	4.290	10.200	1.450	0.700
10.000	987.700	1.320	4.190	8.460	1.113	0.720
15.000	987.100	1.220	4.180	7.095	1.004	0.740
20.000	986.210	1.270	4.180	5.000	1.002	0.750
25.000	985.050	0.708	4.170	4.130	0.332	0.760
30.000	983.650	0.528	4.170	3.410	0.242	0.770
35.000	982.040	0.628	4.170	3.820	0.240	0.785
40.000	980.220	0.528	4.170	2.330	0.237	0.810
45.000	978.220	0.498	4.170	1.910	0.233	0.860
50.000	976.050	0.428	4.170	1.550	0.222	0.660
55.000	973.710	0.248	4.170	1.250	0.202	0.670
60.000	971.210	0.248	4.170	0.980	0.201	0.670
65.000	967.570	0.318	4.180	0.750	0.190	0.680
70.000	963.780	0.368	4.180	0.550	0.180	0.680
75.000	961.860	0.258	4.180	0.370	0.168	0.690
80.000	958.800	0.248	4.200	0.220	0.165	0.690
85.000	954.620	0.328	4.190	0.080	0.157	0.690
90.000	953.320	0.288	4.200	0.210	0.145	0.700
95.000	948.900	0.58	4.200	0.980	0.135	0.700
100.000	944.430	0.228	4.210	0.950	0.114	0.700

Table 2: Dimensions of a triple-tube heat exchanger with ribs

Parameter Description	Measurement (mm)
Thickness of the Ribs (t _R)	2 mm

Distance Between Ribs (λ)	50 mm
Height of the Ribs (H)	9 mm
Diameter of the External Tube	70.66 mm
Material's Thermal Conductivity	200 W/mK
Length of the Heat Exchanger (L)	500 mm
Wall Thickness (t_b)	2.77 mm
Inner Tubes' Diameters	13.51 mm
Tube and Rib Material	Aluminum
Diameter of Middle Tubes	45.26 mm

A. CFD analysis

Computational Fluid Dynamics is the apt application and powerful engineering tool that simulates fluid flow and heat transfer processes within a complex system. It produces mathematical models and analytical solutions of numerical algorithms to assist the engineering and scientific community in studying designs, predicting system behavior, and making challenging decisions in aerospace, environmental science, and thermal management fields. By discretizing governing equations such as continuity, momentum, and energy, this allows CFD to study phenomena that would otherwise be impossible or difficult to view directly. The work here is focused on the concentric triple-tube heat exchanger, with fundamental equations in Ansys Fluent used to optimize performance and further deepen the understanding of fluid dynamics in heat transfer systems. The three stages in the CFD analysis process include pre-processing, where a CAD model is created, the mesh is generated, and materials are defined; solution processing, wherein the computer solves the governing equations using the finite element method; and post-processing, whereby the results of the entire model can be reviewed and analysed, thus providing the critical insights regarding system performance.

B. CFD analysis algorithm

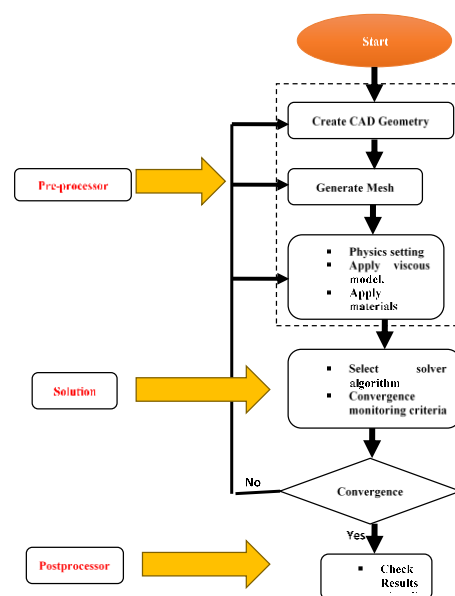


Figure 6: CFD analysis algorithm

C. Governing Equations

This CFD analysis presents a fluid behavior model under steady state, whereby it assumes that the nanofluid has homogeneity with constant properties and acts as an incompressible fluid with constant density. The research is actually concerned with turbulent flow, which is described as disturbed motion-the partial differential equations will again be invoked for continuity, momentum, and energy. The continuity equation guarantees mass conservation, which is represented as $\frac{\partial u_i}{\partial x_i} = 0$ is μ velocity and x_i is spatial coordinates. Momentum conservation is described by the Navier-Stokes equations, which include pressure gradients, viscous effects, and turbulence. The energy equation represents thermal transport, including molecular (T) and turbulent (T_t) thermal diffusivity terms. These equations form a basis for fluid dynamics and heat transfer simulation in the system.

The RNG ($k - \epsilon$) model is used, which considers swirling flows and is more accurate than the standard ($k - \epsilon$) model. The transport equations for the turbulence kinetic energy

(k) and dissipation rate (ϵ) include terms such as velocity gradients, effective viscosity μ_{eff} , and constants like C_μ . The two components of entropy generation are the thermal (S_h) and frictional components, with the total rate expressed as (S_f). Entropy generation is correlated with exergy destruction, with (S_t), which places a great importance on minimizing entropy to ensure better efficiency and a sustainable use of energy sources. These equations permit detailed modelling of fluid behavior and heat transfer, and consequently, optimization of thermal systems is made possible.

D. Exploring the Concentric Triple-Tube Heat Exchanger through Computational Fluid Dynamics Analysis:

• Concentric Triple-Tube Heat Exchanger CAD Model Without Baffle

In this study, a detailed 3D CAD model of a concentric triple tube heat exchanger was designed using ANSYS Workbench, featuring a straight baffle arrangement to enhance heat transfer efficiency. The heat exchanger comprises three tubes with diameters of 13.51 mm, 45.26 mm, and 70.66 mm for the inner, middle, and outer tubes, respectively, forming a complex geometry optimized for performance analysis. Mesh generation, an essential step in CFD analysis, was conducted to divide the geometry into 2,243,493 nodes and 2,580,394 elements, including Tet4, Hex8, and Wed6 element types, with an element size of 0.5 mm. This meticulous modelling and meshing lay the groundwork for in-depth computational simulations and performance optimization.

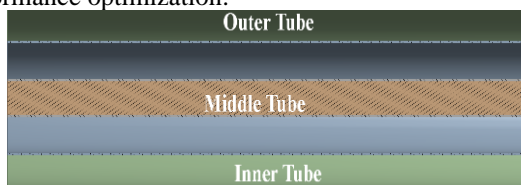


Figure 7: Concentric tube triple tube heat exchanger without baffles in CAD model



Figure 8: Mesh Generation for Triple-Concentric Tube Heat Exchanger with Straight Baffles

• CAD Model of Concentric Triple-Tube Heat Exchanger with Straight Baffle:

In this study, a detailed 3D CAD model of a concentric triple-tube heat exchanger with a straight baffle was meticulously created using the advanced design module of ANSYS Workbench. This highly accurate and detailed representation forms the basis for comprehensive analysis and evaluation of the heat exchanger's design and thermal performance. The model features a baffle height of 9 mm, with baffles spaced 50 mm apart, as shown in Figure 4.4. The heat exchanger comprises inner, intermediate, and outer tubes with diameters of 13.51 mm, 45.26 mm, and 70.66 mm, respectively, and a length of 500 mm. During the

meshing phase, depicted in Figure 5.5, the geometry was subdivided into 3,059,523 elements and 3,918,427 nodes using Tet4, Hex8, and Wed6 element types, each with a 0.5 mm element size, ensuring precision in subsequent CFD simulations.

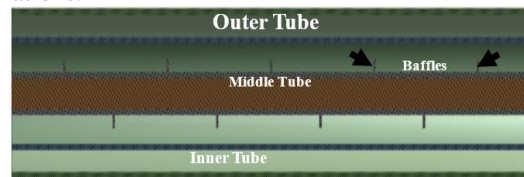


Figure 9: CAD model for concentric tube triple tube heat exchanger with straight baffles

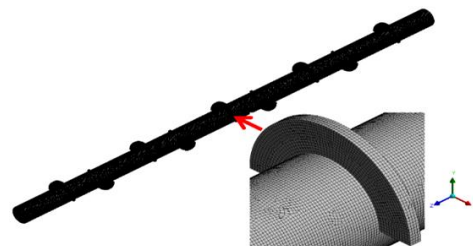


Figure 10: Meshing of concentric tube triple tube heat exchanger with straight baffles

• CAD model of concentric triple tube heat exchanger with inclined baffles at 45°:

In this research, a highly precise 3D CAD model of a concentric triple-tube heat exchanger with inclined baffles was developed using the advanced design module of ANSYS Workbench. This model faithfully represents the physical structure and intricate geometrical details necessary for conducting accurate simulations and in-depth analyses. The heat exchanger features inclined baffles at a 45-degree angle, spaced 50 mm apart, with tube diameters of 13.51 mm (inner), 45.26 mm (intermediate), and 70.66 mm (outer), and a length of 500 mm, as illustrated in Figure 4.6. This detailed modeling ensures reliable scrutiny of fluid flow patterns, heat transfer mechanisms, and overall thermal performance, enabling potential design optimizations. The meshing phase, depicted in Figure 5.7, resulted in 3,918,427 nodes and 3,059,523 elements, comprising Tet4, Hex8, and Wed6 element types with an element size of 0.5 mm, further enhancing simulation accuracy and computational precision.

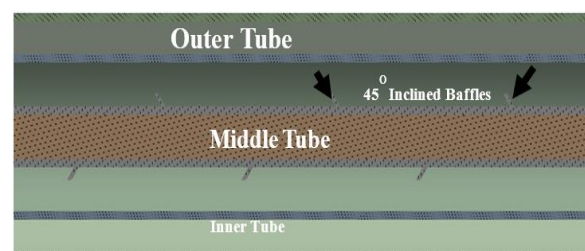


Figure 11: CAD Model of a Triple-Tube Heat Exchanger with Concentric Tubes and 45° Inclined Baffles

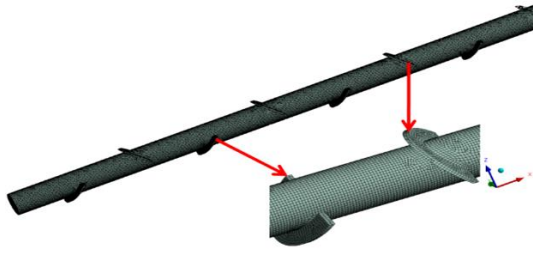


Figure 12: Mesh Generation for Triple-Tube Heat Exchanger with Concentric Tubes and 45° Inclined Baffles

E. Preparation of nanofluid

The graphene nanoplatelets-platinum must first be dispersed in distilled water due to their non-hydrophilic nature. An effective method for achieving this goal is to functionalize GNPs via acid treatment, which helps to introduce functional groups like carboxyl and hydroxyl ones on the surfaces of GNPs.

Table 3: Thermo physical properties of graphene nanoplatelets–platinum nano-fluid

ϕ (%)	Density (kg/m ³)	Specific heat (J/kgK)	Viscosity (kg/ms)	Thermal conductivity (W/mK)
0	1086.05- 0.2970T	0.13T+ 4066.8	$30821240404493.30 \times T^{-6.6681}$	0.002035T- 0.0058
0.1	1087.5- 0.2980T	1.04T+ 3493.5	$351970109.26 \times T^{-4.63845}$	0.0033T- 0.2647

Where ϕ = volume concentration

Table 4: Calculated range for thermo physical properties of nano-fluid

ϕ (%)	Density (kg/m ³)	Specific heat (J/kgK)	Viscosity (kg/ms)	Thermal conductivity (W/mK)	Prandelt number $P_r = \frac{C_p \cdot \mu}{k}$
0	1086.05 -102.8367	4066.8-41.16	0.00038307	0.697663-0.0058	0.0111-0.0090
0.1	1087.5- 103.1797	350.86-3492.5	0.00061190	1.0977-0.02647	0.2351-0.0566

As it enters the inner tube, the temperature of the graphene nanoplatelets-platinum nanofluid is set at 343 Kelvin (K). The starting point for our investigation into the heat transfer dynamics of the nanofluid within the heat exchanger system is this particular temperature setting, which acts as the fundamental thermal condition at the entrance of the inner tube and forms a crucial parameter in our analysis.

• Calculation of mass flow rate

The Reynolds no. of nano-fluid is assumed as 5000
Cross sectional area of tube where hot nano-fluid flowing is $\pi(r_2^2 - r_1^2)$

$$v = \frac{0.001466 \text{ m}^2 \cdot R_e \times \mu}{\rho \times (r_2 - r_1)}$$

Table 5: Calculated value of Linear velocity and mass flow rate for nano-fluid

ϕ (%)	Density(ρ) (kg/m ³)	Viscosity (μ) (kg/ms)	Velocity (m/sec) $v = \frac{R_e \times \mu}{\rho \times (r_2 - r_1)}$	Mass flow rate $\dot{m} = \rho \times A \times v$ (Kg/Sec)
0	1086.05 -102.8367	0.00038306	0.1113-1.1848	0.017296
0.1	1087.5- 103.1797	0.00061190	0.1775-1.8863	0.027628

F. Boundary conditions

With Fluent software, the CFD analysis was performed in such a way that, through energy equations, temperature distribution was achieved and applied, while the RNG k-epsilon model was applied to simulate turbulence precisely with whirling effects. The heat exchanger, made up of aluminium, used graphene nanoplatelets and platinum nanofluid at different concentrations (0.0 and 0.1). The outer tube was insulated for adiabatic conditions, and heat transfer was facilitated due to ribbed inner and intermediate walls of the tube. The cold and normal fluid inlets had temperatures of 283 K and 291 K with a mass flow rate of 0.1 kg/sec, whereas the nanofluid inlet was at a Reynolds number of 5000 and varying flow rates based on concentration, with an inlet temperature of 343 K. The outlet gauge pressure was set to zero, and all other surfaces were treated as solid walls with no-slip conditions. The

SIMPLE algorithm combined pressure and velocity, while the second order upwind scheme made sure that there was numerical stability and accuracy for momentum, energy, and turbulence calculations.

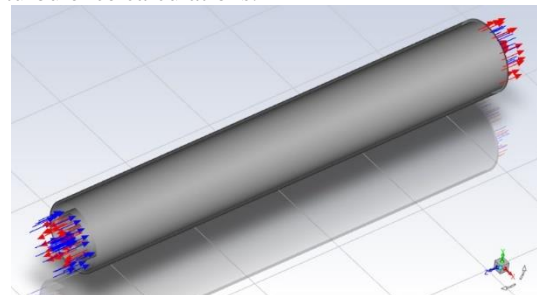


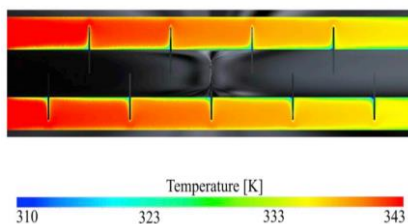
Figure 13: Boundary Condition of concentric tube triple tube heat exchanger with straight baffles

V.RESULT ANALYSIS

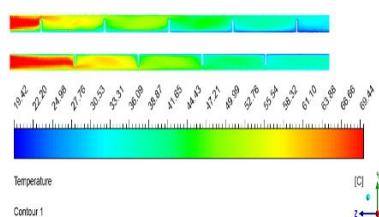
This study employs mathematical techniques and Computational Fluid Dynamics (CFD) to optimize the thermal efficiency of concentric triple-tube heat exchangers with and without baffles, including configurations with straight and 45° inclined baffles. Two cold fluids flow through the innermost and outermost tubes, while a hot fluid flows through the central tube, with nanofluids of varying concentrations (0 and 0.1%) enhancing performance evaluation. An adiabatic condition is maintained to prevent heat loss through the outer tube wall, and Fluent software is used for simulations, leveraging the finite volume method and SIMPLE algorithm for solving fluid flow and heat transfer equations. The RNG *k* turbulence model and second-order upwind scheme ensure precision, capturing intricate flow and thermal behavior, enabling effective optimization of heat exchanger designs.

A. Model validation

A seminal study done by Nima Mazaheri et al. in collaboration with Kermanshah University of Technology analyzed the performance of a ribbed triple-tube heat exchanger using graphene nanoplatelets nanofluid, considering its superior thermal properties through entropy generation and exergy destruction analysis. Based on the above, this research investigated the performance of a concentric triple-tube heat exchanger, with straight baffles, which had a 50 mm spacing and 9 mm height.

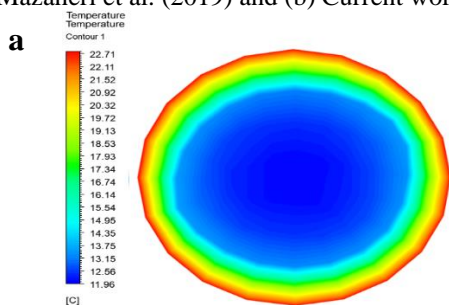


(a) Nima Mazaheri et al (2019)



(b) Current work

Figure 14: Comparing Inner Tube Temperature Distribution at 9 mm Rib Height between (a) Nima Mazaheri et al. (2019) and (b) Current work



With cold water at the innermost tube, normal water at the outermost tube, and nanofluid in the middle tube, considerable temperature fluctuations were experienced at $\phi = 0.1$, providing new understanding of thermal behavior. The two studies were compared with a 5.96% variation in temperature drop along the tube length as shown in the table below

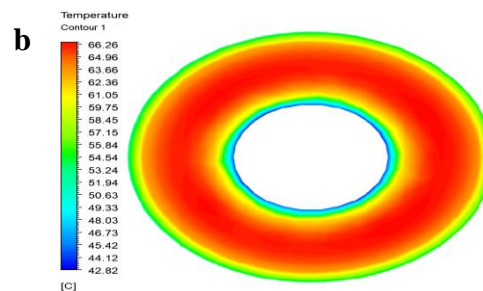
Table 6: Comparative results of maximum and minimum temperature

Minimum temperature		Maximum temperature		Percentage difference	
Nima Mazaheri et al.	Prese nt work	Nima Mazaheri et al.	Prese nt work	Minimu m temperat ure	Maximu m temperat ure
310	292.57	343	342.55	5.96%	0.185%

This study continues the work of Mehdi Bahiraei et al., who investigated configurations without baffles, with straight baffles, and with 45° angled baffles for a range of concentration ratios.

• Concentric triple tube heat exchanger analysis with no baffle at 0.0% nano-fluid concentration

A detailed CFD analysis of a concentric triple-tube heat exchanger was conducted to evaluate the impact of baffle-less operation and $\phi = 0.0\%$ nanofluid concentration on thermal performance. Initial inlet temperatures were precisely set, with cold water at 11.96°C, nanofluid at 42.82°C, and normal water at 18.80°C, establishing baseline conditions. The system, operating with a starting temperature of 9.85°C, demonstrated intricate heat transfer dynamics, achieving an overall outlet temperature of 69.36°C. Specifically, the outlet temperatures for cold water, nanofluid, and normal water were 22.71°C, 66.26°C, and 41.96°C, respectively, reflecting the system's heat exchange efficiency. Contours figure 15 highlighted a temperature variation between 9.85°C and 69.36°C across the tubes, showcasing the thermal characteristics of the exchanger. These findings provide valuable insights into the heat transfer mechanisms and optimization strategies, contributing to the broader understanding of heat exchanger performance in industrial application.



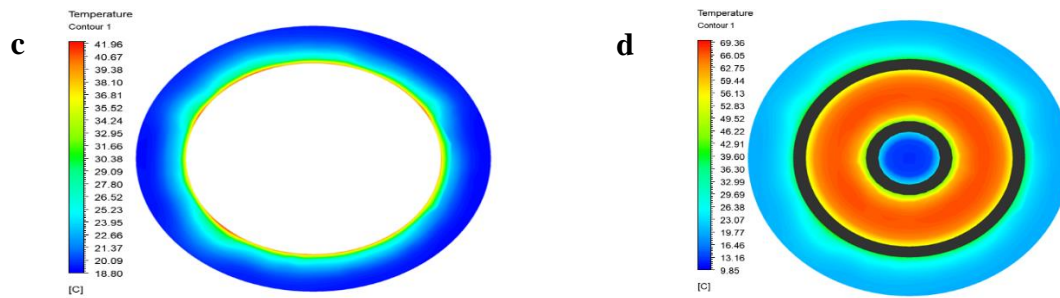


Figure 15: Temperature at outlet for concentric triple tube heat exchanger without baffle at $\phi = 0.0\%$ nano-fluid concentration: a) cold outlet, b) Nano-fluid Outlet, c) Normal water outlet and d) concentric triple tube

• **CFD analysis of the concentric triple tube heat exchanger without baffle at 0.1% concentration of nano-fluid:**

The thermal behavior of a concentric triple-tube heat exchanger without baffles was investigated at a nanofluid concentration (ϕ) of 0.1% through a CFD analysis. Initial inlet temperatures were recorded as 10.69°C for cold water, 19.85°C for nanofluid, 18.22°C for normal water, and

10.69°C for the triple-tube. Outlet temperatures indicated a good heat transfer process, where cold water had 20.04°C, nanofluid had 41.80°C, normal water had 36.91°C, and the triple-tube had 41.71°C. Contours figure 16 presented a temperature range of 10.69°C to 41.80°C, which indicates the capability of nanofluids to improve thermal efficiency and provides knowledge for the improvement of industrial heat exchangers.

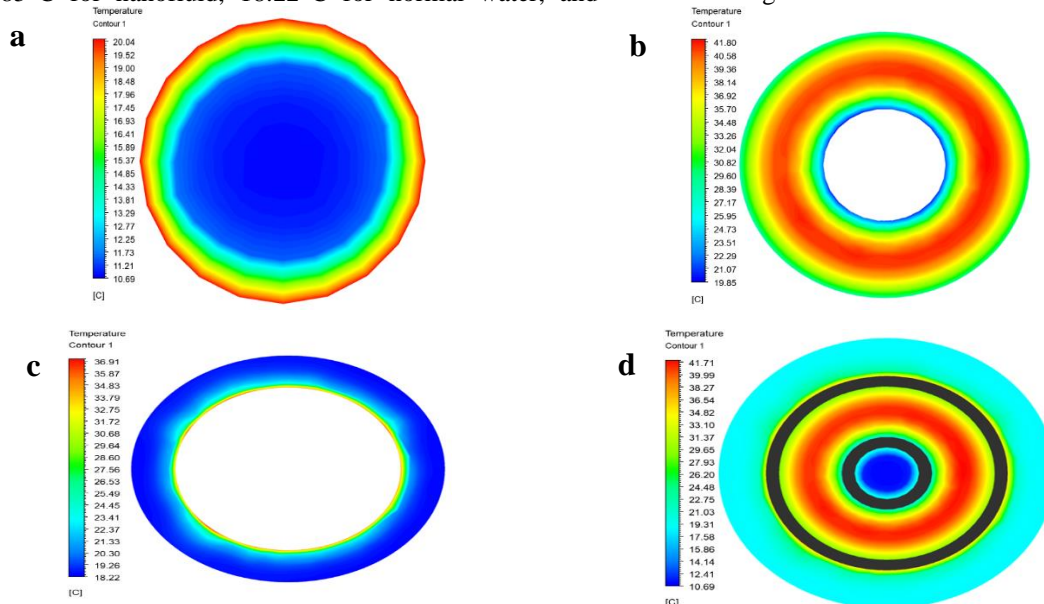


Figure 16: Temperature at outlet for concentric triple tube heat exchanger without baffle at $\phi = 0.1\%$ nano-fluid concentration: a) cold outlet, b) Nano-fluid Outlet, c) Normal water outlet and d) concentric triple tube

• **CFD analysis for concentric triple tube heat exchanger with straight baffle at 0.0% nano-fluid concentration**

We measured the inlet temperatures of cold water (13.38°C), nano-fluid (50.86°C), normal water (19.54°C), and the concentric triple-tube (13.38°C) after performing

CFD analysis on a straight-baffled, $\phi = 0.0\%$ nanofluid heat exchanger. The temperatures for cold water, nanofluid, and normal water were 28.15°C, 65.19°C, and 46.52°C, respectively, at the outlets, while the temperature for the concentric triple-tube's outlet was 64.85°C. According to Contours figure 17, the total temperature range for all tubes was between 13.38°C and 65.19°C.

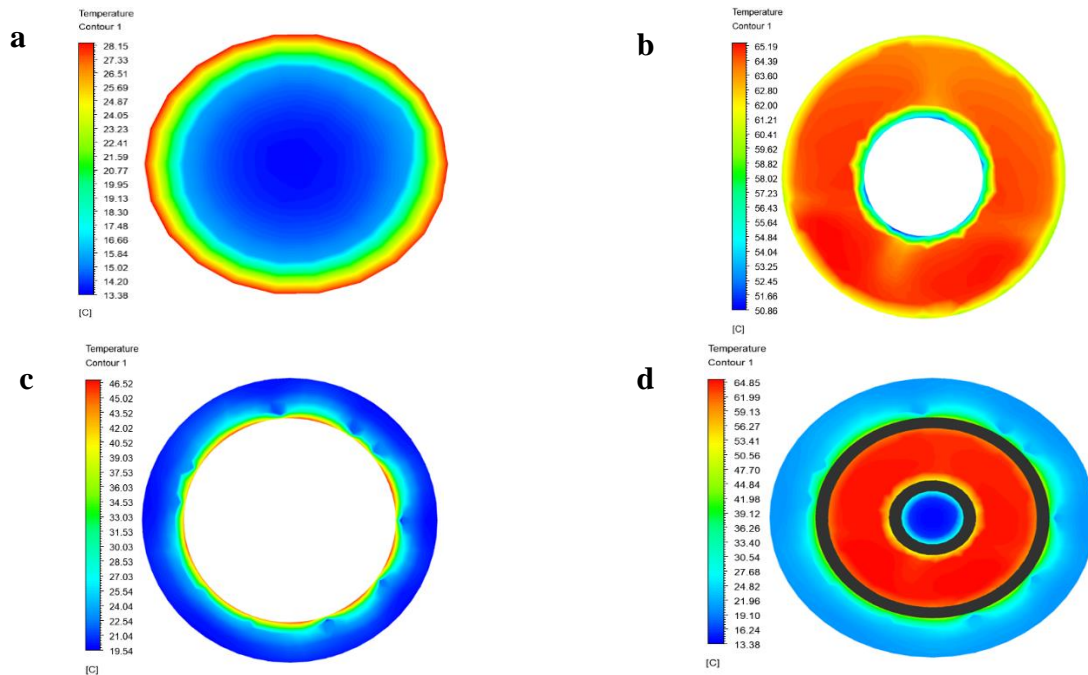


Figure 17: Temperature at outlet for concentric triple tube heat exchanger with straight baffle at $\phi = 0.0\%$ nano-fluid concentration: a) cold outlet, b) Nano-fluid Outlet, c) Normal water outlet and d) concentric triple tube

• **CFD analysis for concentric triple tube heat exchanger with straight baffle at 0.1% nano-fluid concentration:**

After a computational fluid dynamics analysis of a concentric triple-tube heat exchanger with a straight baffle and a $\phi=0.1\%$ nanofluid concentration, the inlet temperatures recorded were: cold water (11.49°C),

nanofluid (23.69°C), normal water (18.17°C), and the concentric triple-tube (11.49°C). The temperatures for cold water, nano-fluid, and normal water were 24.13°C, 37.31°C, and 41.43°C, respectively, at the outlets, while the temperature for the concentric triple-tube's outlet was 41.00°C. According to Contours figure 18, the total temperature range for all tubes was between 11.49°C and 41.43°C.

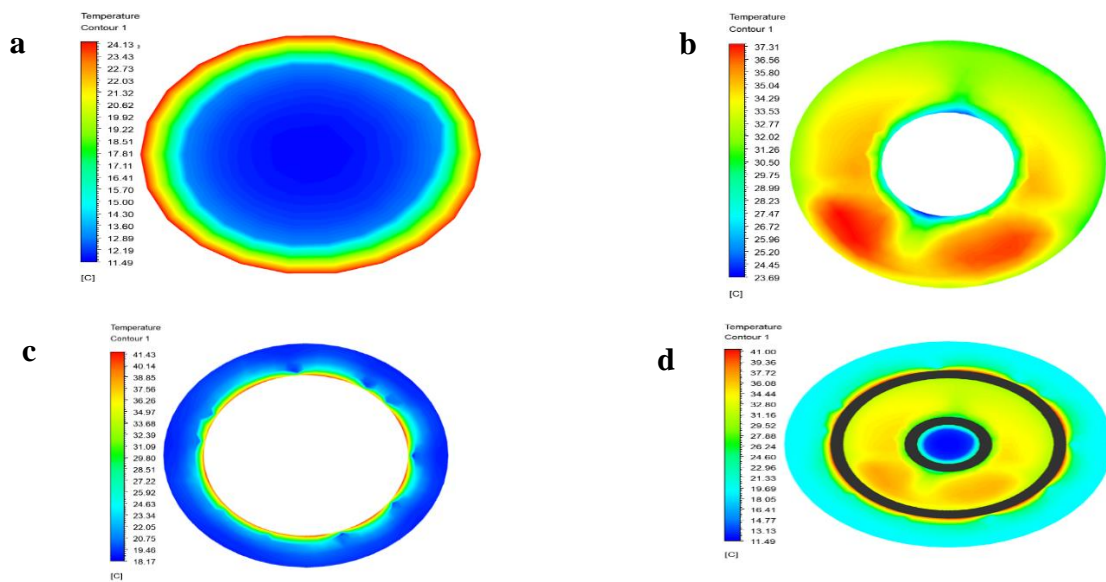


Figure 18: Temperature at outlet for concentric triple tube heat exchanger with straight baffle at $\phi = 0.1\%$ nano-fluid concentration: a) cold outlet, b) Nano-fluid Outlet, c) Normal water outlet and d) concentric triple tube

• **Computational fluid dynamics analysis for concentric triple tube heat exchanger with 45° inclined baffle at 0.0% nano-fluid concentration:**

In the quest for a holistic insight into thermal performance in the context of a heat exchanger system, we conducted a detailed CFD analysis. The specific configuration being

investigated was a concentric triple-tube heat exchanger with a 45° inclined baffle and a nano-fluid concentration parameter set at 0.0%. These intentional design and fluid selection choices were made so that the effect of important variables could be teased out and studied in terms of their singular contributions to the overall phenomenon of heat

transfer. The inlet temperatures captured provide a snapshot of initial thermal conditions at entry points in the system. At an entrance temperature of 12.01°C, nano-fluid, with a variable of immense interest, was brought in at a temperature of 48.29°C, normal water, at a benchmark entered at 21.78°C, and concentric triple-tube heat exchanger itself entered with the initial temperature being 12.00°C. These temperature points give a sound basis for analyzing the ability of the system to enable efficient heat

transfer, thus offering a basis to gain insight into the thermal dynamics at play, which will help inform the potential for optimization and real-world application of this heat exchanger configuration. Cold water, nanofluid, and normal water were all at their respective outlets at 34.02°C, 64.93°C, and 48.28°C, respectively, while the concentric triple-tube's outlet temperature was 64.60°C. The total temperature range for all tubes is as depicted in Contours Diagram 5.18, ranging from 12 to 64.93 degrees Celsius.

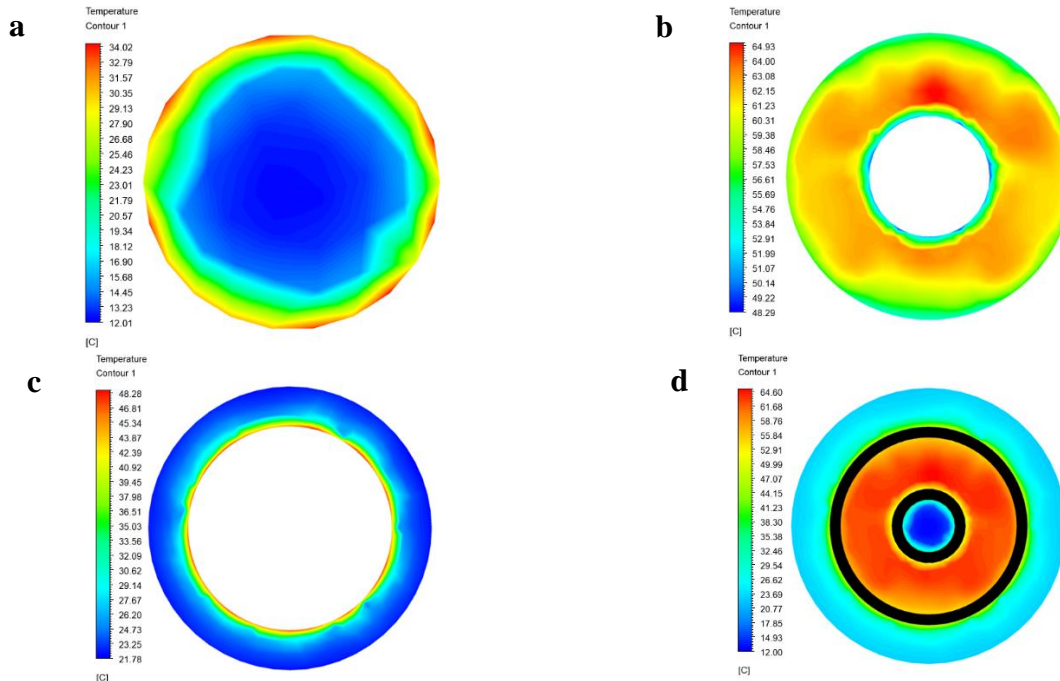
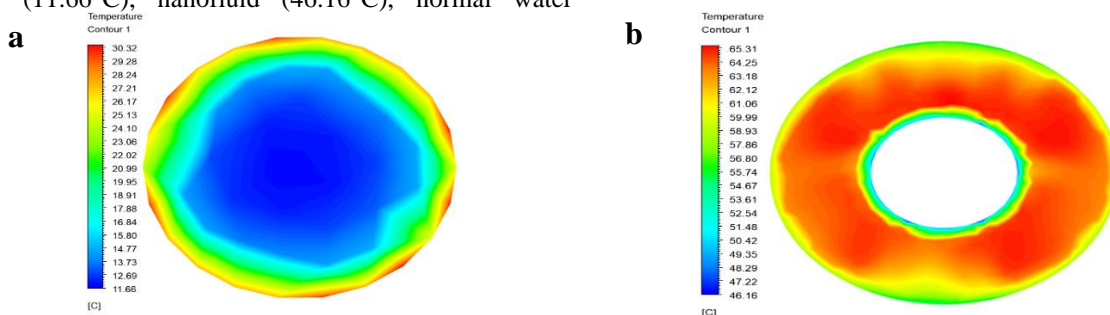


Figure 19: Temperature at outlet for concentric triple tube heat exchanger with 45° inclined baffle at 0.0% nano-fluid concentration: a) cold outlet, b) Nano-fluid Outlet, c) Normal water outlet and d) concentric triple tube

• **CFD Investigation of Concentric Triple-Tube Heat Exchanger with 45° Inclined Baffle and 0.1% Nanofluid Concentration**

Following a CFD analysis on a concentric triple-tube heat exchanger with a 45° inclined baffle and a $\phi=0.1\%$ nanofluid concentration, the inlet temperatures were: cold water (11.66°C), nanofluid (46.16°C), normal water

(18.48°C), and the concentric triple-tube (11.66°C). Cold water, nanofluid, and normal water were all measured at their outlets at 30.32°C, 65.31°C, and 44.67°C, respectively, while the concentric triple-tube had an outlet temperature of 64.99°C. According to Contours figure 20, the average temperature across all tubes was 11.66 to 65.31 degrees Celsius.



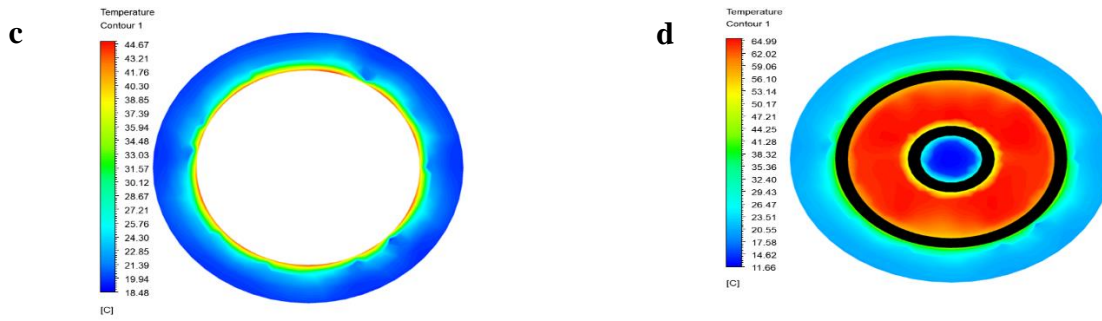


Figure 20: Inlet Temperature Analysis of a Concentric Triple-Tube Heat Exchanger with a 45° Inclined Baffle Using 0.1% Nano-fluid Concentration. a) cold outlet, b) Nano-fluid Outlet, c) Normal water outlet and d) concentric triple tube

B. Temperature Variation Analysis in a Baffle-Free Concentric Triple Tube Heat Exchanger Across Different Concentration Ratios

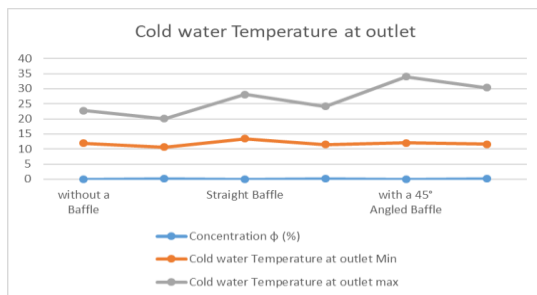


Figure 21: Cold water Temperature at outlet

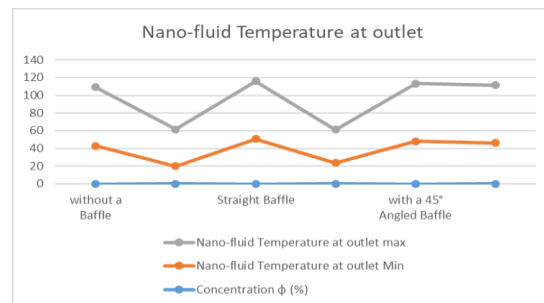


Figure 22: Nano-fluid Temperature at outlet

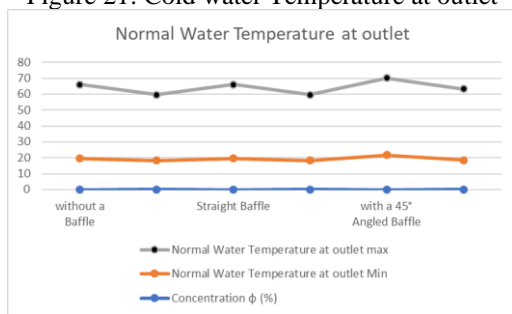


Figure 23: Normal Water Temperature at outlet

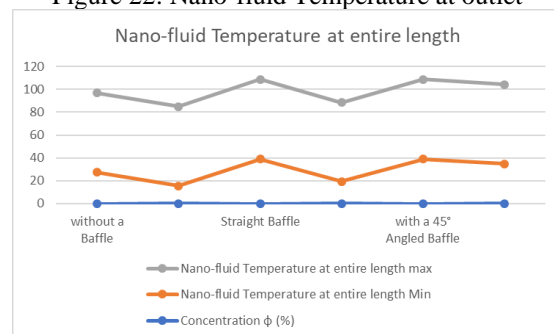


Figure 24: Nano-fluid Temperature at entire length

Table 7: Heat Transfer Rates for the Hot Nanofluid, Cold Fluid, and Normal Fluid

Parameter	ϕ (%)	Cold water Temperature [K]		Nano-fluid Temperature [K]		Normal Water Temperature [K]		Mass flow rate Kg/Sec
		In	out	out	in	in	out	
without baffle	0	283	295.86	315.97	343	291	315.11	0.01730
	0.1	283	293.24	293.00	343	291	310.06	0.02763
straight baffle	0	283	301.30	324.01	343	291	319.67	0.01730
	0.1	283	297.40	296.84	343	291	314.58	0.02763
Baffle inclined at 45o	0	283	307.17	321.45	343	291	321.43	0.01730
	0.1	283	303.48	319.31	343	291	317.82	0.02763

Table 8: Comparison of Heat Transfer Rates and Specific Heat for Various Baffle Configurations in a Triple-Tube Heat Exchanger

Parameter	ϕ (%)	Specific heat [J/kgK]	Heat transfer rate for q_{nf} [watt]	Heat transfer rate for q_{cold} [watt]	Heat transfer rate for q_{normal} [watt]
without baffle	0	4065.8	1900.696	904.290	1695.367
	0.1	3492.5	4824.365	988.030	1839.048

straight baffle	0	4065.8	1335.339	1286.820	2016.017
	0.1	3492.5	4453.854	1389.417	2275.170
Baffle inclined at 45o	0	4065.8	1515.634	1699.727	2139.777
	0.1	3492.5	2285.688	1975.867	2587.982

Table 9: The typical LMTD and overall heat transfer coefficient for various TTHE designs and concentrations

Parameter	without baffle		straight baffle		Baffle inclined at 45°	
	0.0	0.1	0.0	0.1	0.0	0.1
LMTD _{normal & cold}	13.4323	8.9615	19.7668	13.7747	23.7152	21.7718
LMTD _{normalt & nf}	25.4031	10.0439	26.8906	13.2698	27.7536	26.7139
LMTD _{avg}	18.4177	9.5027	22.3287	14.0223	24.7344	24.2428
Overall heat transfer coefficient [w/m ² K]	62599.77	303331.27	34440.25	212239.89	30174.12	64313.10

Table 10 Effectiveness for various TTHE designs at various concentrations

Parameter	φ (%)	Mass flow rate	Specific heat	q _h	q _{max}	Effectiveness
without baffle	0	0.01730	4065.8	1900.696	4219.081	0.4505
	0.02	0.02034	4246.2	2334.114	5183.082	0.4503
	0.06	0.02714	2248.1	1965.491	3660.132	0.5370
	0.1	0.02763	3492.5	4824.365	5789.238	0.8333
straight baffle	0	0.01730	4065.8	1335.339	4219.081	0.3165
	0.02	0.02034	4246.2	1828.764	5183.082	0.3528
	0.06	0.02714	2248.1	1470.153	3660.132	0.4017
	0.1	0.02763	3492.5	4453.854	5789.238	0.7693
Baffle inclined at 45o	0	0.01730	4065.8	1515.634	4219.081	0.3592
	0.02	0.02034	4246.2	1879.817	5183.082	0.3627
	0.06	0.02714	2248.1	1536.340	3660.132	0.4198
	0.1	0.02763	3492.5	2285.688	5789.238	0.3948

Table 11: Bulk mean temperature for various TTHE designs at various concentrations

Parameter	φ (%)	Bulk mean temperature of cold water	Bulk mean temperature of nano-fluid	Bulk mean temperature of normal water
without baffle	0	289.43	329.49	303.06
	0.02	288.90	329.49	302.56
	0.06	289.02	326.89	302.22
	0.1	288.12	318.00	300.53
straight baffle	0	292.15	333.51	305.34
	0.02	291.25	332.42	304.80
	0.06	292.05	330.95	305.15
	0.1	290.20	319.92	302.79
Baffle inclined at 45°	0	295.09	332.22	306.22
	0.02	294.17	332.12	305.72
	0.06	294.34	330.41	305.09

	0.1	293.24	331.16	304.41
--	-----	--------	--------	--------

VI. CONCLUSION

The CFD analysis showed that performance of the heat exchanger significantly depends on both the baffle configurations and the concentrations of nanofluids. Among the cases considered, those with baffle-less, straight, and 45° inclined configurations, the baffle design presented the highest efficiencies. This occurred because the turbulence and temperature gradient were optimized as a result of the inclined baffles, therefore increasing the significant heat transfer rate. The analysis also proved the critical role of nanofluids in improving efficiency in the heat exchanger. With the concentration of the nanofluid set to 0.1%, the system showed outstanding improvement in heat transfer due to the better thermal conductivity properties of the graphene nanoplatelets combined with platinum nanofluid. These results emphasize the effectiveness of combining advanced baffle designs and nanofluids to achieve higher thermal efficiency. In particular, 45° inclined baffles have shown to provide significant benefits in maintaining consistent temperature gradients and enhancing better fluid mixing, leading to better heat exchange capabilities. The study provides valuable insights into designing and optimizing heat exchanger configurations for energy-intensive sectors, providing solutions to enhance energy efficiency and thermal management. The results of this study can be expanded further in the future by trying other nanofluid compositions with different thermal properties and introducing innovative geometric alterations to enhance the performance. These enhancements can lead the way to making more efficient and environmentally friendly heat exchanger systems, where the demand is increasing for optimum thermal energy utilization in various industries.

Conflict of Interest: The corresponding author, on behalf of all authors, confirms that there are no conflicts of interest to disclose.

Copyright: © 2023 by Vikash Singh Patel, Dr. Ankit Goyal, Prof. Priyavrat Kumar Author(s) retain the copyright of their original work while granting publication rights to the journal.

License: This work is licensed under a Creative Commons Attribution 4.0 International License, allowing others to distribute, remix, adapt, and build upon it, even for commercial.

References

- [1] GaneshKumar, P., VinothKumar, S., Vigneswaran, V. S., Kim, S. C., & Ramkumar, V. (2024). Advancing heat exchangers for energy storage: A comprehensive review of methods and techniques. *Journal of Energy Storage*, 99, 113334. <https://doi.org/10.1016/j.est.2024.113334>
- [2] Kirschstein, X., Ohagen, M., Reber, J., Vardon, P. J., & Bishara, N. (2024). Regeneration of shallow borehole heat exchanger fields: a literature review. *Energy and Buildings*, 114381. <https://doi.org/10.1016/j.enbuild.2024.114381>
- [3] Babar, H., Wu, H., Zhang, W., Shah, T. R., McCluskey, D., & Zhou, C. (2024). The promise of nanofluids: A bibliometric journey through advanced heat transfer fluids in heat exchanger tubes. *Advances in Colloid and Interface Science*, 103112. <https://doi.org/10.1016/j.cis.2024.103112>
- [4] Li, M., Wang, J., Chen, Z., Qian, X., Sun, C., Gan, D., ... & Li, X. (2024). A Comprehensive Review of Thermal Management in Solid Oxide Fuel Cells: Focus on Burners, Heat Exchangers, and Strategies. *Energies*, 17(5), 1005. <https://doi.org/10.3390/en17051005>
- [5] Hou, Z., Yang, C., Wang, H., & Li, H. (2024). Heat transfer characteristics and optimization strategies in supercritical fluid heat exchangers with non-uniform thermal boundaries: A systematic review. *International Journal of Heat and Fluid Flow*, 110, 109582. <https://doi.org/10.1016/j.ijheatfluidflow.2024.109582>
- [6] Roudbari, F. N., Ehsani, H., Amiri, S. R., Samadani, A., Shabani, S., & Khodadad, A. (2024). Advances in photovoltaic thermal systems: A comprehensive review of CPVT and PVT technologies. *Solar Energy Materials and Solar Cells*, 276, 113070. <https://doi.org/10.1016/j.solmat.2024.113070>
- [7] Hanafi, M & Bahreinineja, Ardeshir & Uddin, Naseem. (2021). Optimization of shell and tube heat exchanger using the water cycle algorithm. *IOP Conference Series: Materials Science and Engineering*. 1173. 012005. 10.1088/1757-899X/1173/1/012005.
- [8] Porgar, S., Humnic, G., Humnic, A., Najibolashrafi, R., & Salehfehr, S. (2024). Application of nanofluids in heat exchangers-A state-of-the-art review. *International Journal of Thermofluids*, 100945. <https://doi.org/10.1016/j.ijft.2024.100945>
- [9] Wang, X., Zhou, Y., Yao, W., Xia, Y., Xu, T., Yang, H., ... & Gao, W. (2024). The challenge of the ground heat Exchangers: A review of heat transfer efficiency. *Energy Conversion and Management*, 302, 118115. <https://doi.org/10.1016/j.enconman.2024.118115>
- [10] Choure, B. K., Alam, T., & Kumar, R. (2024). Optimization of heat transfer in PCM based triple tube heat exchanger using multitudinous fins and eccentric tube. *Journal of Energy Storage*, 102, 113981. <https://doi.org/10.1016/j.est.2024.113981>
- [11] Ko, Y. M., Song, J. Y., Lee, J. W., Sohn, S., Song, C. H., Khoshvaght-Aliabadi, M., ... & Kang, Y. T. (2024). A critical review on Colburn j-factor and f-factor and energy performance analysis for finned tube heat exchangers. *Energy*, 287, 129609. <https://doi.org/10.1016/j.energy.2023.129609>
- [12] Touatit, Achour & Bougriou, Cherif. (2018). Optimal diameters of triple concentric-tube heat exchangers. *International Journal of Heat and Technology*. 36. 367-375. 10.18280/ijht.360149.

- [13] Kolo, I., Brown, C. S., Nibbs, W., Cai, W., Falcone, G., Nagel, T., & Chen, C. (2024). A comprehensive review of deep borehole heat exchangers (DBHEs): subsurface modelling studies and applications. *Geothermal Energy*, 12(1), 19. <https://doi.org/10.1186/s40517-024-00297-3>
- [14] Amanuel, Tarikayehu & Mishra, Manish. (2018). Thermohydraulic optimization of triple concentric-tube heat exchanger: A multi-objective approach. Proceedings of the Institution of Mechanical Engineers, Part E: Journal of Process Mechanical Engineering. 233. 095440891877923. 10.1177/0954408918779232.
- [15] A. Afzal, A.D.M. Samee, R.K.A. Razak, and M.K. Ramis, "Heat transfer characteristics of MWCNT nanofluid in rectangular mini channels", *Int J Heat Technol.*, Vol. 36, Pp. 222–228, 2018. <https://doi.org/10.18280/ijht.360130>
- [16] A. Afzal, I. Nawfal, I.M. Mahbulbul, and S.S. Kumbar, "An overview on the effect of ultrasonication duration on different properties of nanofluids", *J. Therm. Anal. Calorim.*, 2018. <https://doi.org/10.1007/s10973-018-7144-8>.
- [17] A. Afzal, AD MS, RK AR, "Experimental Thermal Investigation of CuO-W Nanofluid in Circular Minichannel", *Model Meas Control B.*, Vol. 86, Pp. 335–344, 2017.
- [18] S. Rashidi, M.H. Kashefi, K.C. Kim, and O. Samimi-Abianeh, "Potentials of porous materials for energy management in heat exchangers—A comprehensive review", *Appl. Energy*, Vol. 243, Pp. 206–232, 2019.
- [19] Sumit Kr. Singh & Jahar Sarkar (2020) "Improving hydrothermal performance of hybrid nanofluid in double tube heat exchanger using tapered wire coil turbulator" *Advanced Powder Technology* 3 March 2020 <https://doi.org/10.1016/j.apt.2020.03.002>.
- [20] B.V.N. Ramakumar, J.D. Arsha, P. Tayal, Tapered twisted tape inserts for enhanced heat transfer, *J. Heat Transf.* 138 (2016) 1–9.
- [21] M.E. Nakhchi, J.A. Esfahani, Numerical investigation of turbulent Cu-water nanofluid in heat exchanger tube equipped with perforated conical rings, *Adv. Powder Technol.* 30 (2019) 1338–1347.
- [22] S.K. Singh, J. Sarkar, Improving hydrothermal performance of double-tube heat exchanger with modified twisted tape inserts using hybrid nanofluid, *J. Therm. Anal. Calorimetry* (2020), <https://doi.org/10.1007/s10973-020-09380-w>
- [23] P Tanish et al (2021) "Experimental Study of Heat Transfer in Concentric Triple Pipe Heat Exchanger" *Materials Science and Engineering* 1130 (2021) 012048 doi:10.1088/1757-899X/1130/1/012048.
- [24] Malika, M., & Sonawane, S. S. (2024). Ecological optimization and LCA of TiO₂-SiC/water hybrid nanofluid in a shell and tube heat exchanger by ANN. *Proceedings of the Institution of Mechanical Engineers, Part E: Journal of Process Mechanical Engineering*, 238(1), 45-55. <https://doi.org/10.1177/09544089221093304>
- [25] Abdollahpour, M. S., & Darbandi, M. (2024). Developing an algorithm to evaluate the tube and baffle choice influences on enhancing the hydrothermal performances of shell and tube heat exchangers. *International Journal of Heat and Mass Transfer*, 222, 125178. <https://doi.org/10.1016/j.ijheatmasstransfer.2024.125178>
- [26] Ghalandari, M., Irandoost Shahrestani, M., Maleki, A., Safdari Shadloo, M., & El Haj Assad, M. (2021). Applications of intelligent methods in various types of heat exchangers: a review. *Journal of Thermal Analysis and Calorimetry*, 1-12. <https://doi.org/10.1007/s10973-020-10425-3>
- [27] Yang, L., Jin, X., Zhang, Y., & Du, K. (2021). Recent development on heat transfer and various applications of phase-change materials. *Journal of cleaner production*, 287, 124432. <https://doi.org/10.1016/j.jclepro.2020.124432>
- [28] Mousa, M. H., Miljkovic, N., & Nawaz, K. (2021). Review of heat transfer enhancement techniques for single phase flows. *Renewable and Sustainable Energy Reviews*, 137, 110566. <https://doi.org/10.1016/j.rser.2020.110566>